Potentiometric, ^{1}H NMR and ESI-MS investigation on dimethyltin(IV) cation–mercaptocarboxylate interaction in aqueous solution†

Paola Cardiano,[a] Ottavia Giuffrè,[a] Anna Napoli[b] and Silvio Sammartano*[a]

Received (in Victoria, Australia) 23rd April 2009, Accepted 14th August 2009
First published as an Advance Article on the web 8th September 2009
DOI: 10.1039/b908114c

The interaction between dimethyltin(IV) cation with three different mercaptocarboxylic acids (thiolactic, 3-mercaptopropanoic and thiomalic acids) was studied in aqueous solution by potentiometry, ^{1}H NMR spectroscopy and electrospray (ESI) mass spectrometry. The speciation model and equilibrium data were determined on the basis of potentiometric evidences, as well as the bonding sites by means of ESI mass spectrometry and the geometry of the species by ^{1}H NMR spectroscopy. The speciation profiles show the formation of different complex species, whose stabilities and formation percentages, in particular for the mononuclear mixed species, are high in a wide pH range. ESI mass spectrometry studies together with ^{1}H NMR investigations fully confirm the speciation model. The former also allows to propose a cyclic structure with O→Sn and S→Sn coordination, confirmed by MS/MS analysis; the latter indicates angles mostly matching with a Tbp arrangement around the metal.

Introduction

The use of organotin(IV) compounds in industrial and agricultural fields as biocides has caused their accumulation in the environment and consequently in biological systems.[1,2] In the natural environment, organotin compounds can also be generated from methylation having an anthropogenic origin.[3] Huey *et al.* first reported that methyltin species can be produced by the addition of inorganic Sn(II) or Sn(IV) to sediments.[4] Since then, inorganic Sn methylation was widely studied and related to microorganism activity.[5–9] Organotin compounds can be absorbed from water onto particulate matter and can be either removed from water into sediments or remain dissolved in the water, where they undergo either degradation processes or can be accumulated by aquatic organisms.[3] The main biochemical pathway affected by diorganotin compounds is the inhibition of α-keto acid oxidation, probably by reacting with enzymes or coenzymes having dithiol groups, such as reduced lipoic acid. The strongest interactions occur between triorganotin compounds and protein residues such as histidine and cysteine, giving species with Sn–S bonds, where Sn shows a tetrahedral or *cis*-pentacoordinate structure. The bioaccumulation process will depend on the lipophilicity of the substance and on its resistance to metabolic and excretory processes.[10]

The characterization of the interactions between organotin moieties and low molecular weight compounds present in biological fluids can be used for modelling the behaviour of macromolecular compounds. The solution equilibrium studies of the organotin and biologically relevant ligands have importance for the potential pharmaceutical application of organotin compounds.[11,12] In fact, besides their toxicity, which reaches a maximum for trialkylsubstituted tin species, organotin compounds have been found to have therapeutic effects on various tumour cells *in vitro*.[13] The recent review of Nath *et al.* also underlines the lack of solution studies regarding the interaction between organotin compounds and biologically relevant ligands, which could give fundamental information on the speciation of organotin(IV) and its bioavailability.[11]

Moreover, few studies report on the binding ability of different S-containing ligands toward dialkyltin(IV) cations and only some of these contain structural information and spectroscopic properties of these complexes in aqueous solution. The established methods used for the structure elucidation of organotin(IV) compounds are nuclear magnetic resonance (NMR) based on ^{1}H, ^{13}C and ^{119}Sn chemical shifts and ^{119}Sn Mössbauer spectroscopy.[14–21] On the other hand, electrospray ionization (ESI) is one of the softest ionization techniques and makes possible to determine the molecular weight of many organometallic[22,23] and metal complex compounds.[24] Most studies were performed on simple organotin compounds[25] and many papers oriented mainly on the synthetic aspects only claim that the structures or MWs are confirmed by ESI-MS without further reasoning. Structural information of organotin(IV) compounds is quite difficult, even under the softest ionization conditions because non-covalent bonds of these compounds can be cleaved during the ionization process, and therefore the molecular adducts may be missing completely, or their relative abundances are very low in the full-scan mass spectra. Furthermore many solvents compete towards cation binding and adduct formation may complicate the interpretation of the mass spectra.

[a] *Dipartimento di Chimica Inorganica, Chimica Analitica e Chimica Fisica, Università di Messina, Salita Sperone 31, Villaggio S. Agata, 98166 Messina, Italy. E-mail: ssammartano@unime.it; Fax: 0039090392827*
[b] *Dipartimento di Chimica, Università della Calabria, Via P. Bucci, 87036 Arcavacata di Rende, Italy*

† Electronic supplementary information (ESI) available: Fig. 1S: Chemical shifts of CH_3 *vs.* pH in dimethyltin(IV)–L 1 : 2 mixtures: (a) L = TLA; (b) L = TMA. See DOI: 10.1039/b908114c

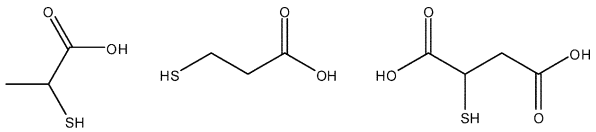

2-mercaptopropanoic acid or thiolactic acid **(TLA)** | 3-mercaptopropanoic acid **(MPA)** | 2-mercaptosuccinic acid or thiomalic acid **(TMA)**

Chart 1

Over the last decade some of us have extensively studied the speciation of alkyltin cations in aqueous solution including the hydrolysis processes in various ionic media at different temperatures, also simulating the composition of natural waters;[26–31] as well as the interactions with ligands of environmental and biological interest, such as polycarboxylates and L-cysteinate.[32–35]

In this work the electrospray ionization (ESI) mass spectrometric approach is exploited for the structure elucidation *in situ* of organotin(IV) complexes in aqueous solution, as obtained at room temperature from simply mixing solutions of dimethyltin(IV) cation and weak ligands, for example mercaptocarboxylic acids, in different conditions of pH and M : L ratios.

The equilibrium behaviour and the speciation model in aqueous solution in a wide pH range, between dimethyltin(IV) and three mercaptocarboxylic acids (Chart 1) and possible structures of the complexes formed will be discussed on the basis of potentiometric, ^{1}H NMR spectroscopic and electrospray mass spectrometric results.

Experimental

Materials

Dimethyltin(IV) was used as its chloride salt ($(CH_3)_2SnCl_2$). The solutions were prepared from Aldrich commercial products twice re-crystallised before use. Mercaptocarboxylate ligands (Fluka or Aldrich) were used without further purification. Their purity (always >99.5%) was checked by potentiometric titration. Hydrochloric acid and sodium hydroxide solutions were prepared by diluting concentrated Fluka ampoules and standardised against sodium carbonate and potassium hydrogen phthalate, respectively. All solutions were prepared by using ultrapure water (conductivity <0.1 μS cm^{-1}) and grade A glassware.

Potentiometric equipment and procedure

Potentiometric titrations were carried out (at 25.0 ± 0.1 °C) using apparatus consisting of a model 713 Metrohm potentiometer, equipped with a combined glass electrode (Ross type 8102, from Orion) and a model 765 Metrohm motorised burette. Estimated accuracy was ±0.2 mV and ±0.003 mL for e.m.f. and titrant volume readings, respectively. The apparatus was connected to a PC, and automatic titrations were performed using a suitable computer program to control titrant delivery, data acquisition and to check for e.m.f. stability. All titrations were carried out under magnetic stirring and presaturated N_2 was bubbled through the purified solution in order to exclude O_2 and CO_2. A volume of 25 ml of the solution containing the ligand under study at C_L = 2–6 mmol L^{-1} and the dimethyltin(IV) cation at C_M = 2–4 mmol L^{-1} was titrated with standard NaOH up to 80–90% neutralization. Independent titrations of HCl with standard NaOH were carried out to determine standard electrode potential E^0 and to obtain pH = −log[H$^+$] readings. All the measurements were performed at very low ionic strength (I = 0.01 mol L^{-1}) to avoid the interference of the supporting electrolyte with both the cation and the anion under study.

Mass spectrometry

Electrospray spectra were obtained in positive or in negative ion mode on a hybrid Q-Star Pulsar-i (MSD Sciex Applied Biosystem, Toronto, Canada) mass spectrometer equipped with an ion spray ionization source. Samples were analyzed by direct infusion (5 μL min^{-1}) of aqueous solutions of **1–3**, **1a–3a** and **1b–3b** at the optimum ion spray (IS) voltage of 4800 V.

The source nitrogen (GS1) and the curtain gas (CUR) flows were set at pressures of 20 and 25 psi, respectively, whereas the first declustering potential (DP1), the focusing potential (FP) and the MS/MS experiments were performed in the collision cell q on the most abundant isotope ^{120}Sn of the selected precursor ions by keeping the first quadrupole analyzer at 20 V relative to ground and operating at unit resolution and scanning the time-of-flight (TOF) analyzer. The collision energy was set at 20 eV, while the gas pressure of the collision chamber was maintained at the instrumental parameters CAD 5, which corresponded to a pressure of the chamber of 6.86 × 10^{-3} Torr and a surface density of 9.55 × 10^{15} molecules cm^{-2}. All the acquisitions were averaged over 60 scans at a TOF resolving power of 8000.

Preparation of MS samples

Stock solutions (A–C) were prepared by dissolving the appropriate amount of the organic acid in water: stock solution A: 5.1 mmol L^{-1} TLA; stock solution B: 4.9 mmol L^{-1} TMA; stock solution C: 5.0 mmol L^{-1} MPA; stock solutions D–G were prepared by mixing solutions A–C and 50 mmol L^{-1} NH_4HCO_3 in 3 : 1 (v/v) ratio.

Samples **1–3** were prepared by adding 600 μL of the stock solutions A–C to 60 μL of an aqueous solution of $(CH_3)_2SnCl_2$ at C_M = 5.1 mmol L^{-1} and directly analyzed by ESI MS in positive ion mode.

Samples **1a–3a** were prepared by adding 600 μL of solutions D–G to 60 μL of an aqueous solution of $(CH_3)_2SnCl_2$ at C_M = 5.1 mmol L^{-1}. To the resulting solution was added *N*,*N*-diisopropylethylamine (DIPEA) (2 μl DIPEA in 100 μL of CH_3CN) until pH ≅ 9.

Samples **1b–3b** were prepared by adding 600 μL of solutions A–C to 60 μL of an aqueous solution of $(CH_3)_2SnCl_2$ at C_M = 5.1 mmol L^{-1}. To the resulting solution was added standard Me_4NOH until pH ≅ 9.

ESI MS and MS/MS data. Ions observed in the full-scan positive and negative ion ESI mass spectra are listed. All m/z values are related to the most abundant natural isotopes, *i.e.* ^{120}Sn isotope for tin atoms.[36] Mass measurements were performed with the accuracy of 10 ppm.

Sample **1**: (+)TOF MS: *m/z* 254.95 $[C_5H_{11}O_2SSn)]^+$, 508.89 $[C_{10}H_{21}O_4S_2Sn_2)]^+$

MS/MS of *m/z* 254.95: *m/z* 236.95 $[C_5H_9OSSn]^+$, 226.95, 208.94 $[C_4H_9SSn]^+$, 181.90 $[C_2H_7SSn]^+$, 166.95 $[C_2H_7OSn]^+$, 150.90 $[C_2H_7Sn]^+$

Sample **2**: (+)TOF MS: *m/z* 298.95 $[C_6H_{11}O_4SSn]^+$, 280.94 $[C_6H_9O_3SSn]^+$, 597.87 $[C_{12}H_{22}O_8S_2Sn_2]^+$.

MS/MS of *m/z* 298.95: *m/z* 280.9 $[C_6H_9O_3SSn]^+$, 252.95 $[C_5H_9O_2SSn]^+$, 240.9 $[C_4H_9O_2SSn]^+$, 208.9 $[C_4H_9SSn]^+$, 166.35 $[C_2H_7OSn]^+$, 150.9 $[C_2H_7Sn]^+$

Sample **3**, (+)TOF MS: *m/z* 254.95 $[C_5H_{11}O_2SSn)]^+$, 508.89 $[C_{10}H_{21}O_4S_2Sn_2)]^+$.

MS/MS of *m/z* 254.95: *m/z* 236.95 $[C_5H_9OSSn]^+$, 226.95, 208.94 $[C_4H_9SSn]^+$, 181.9 $[C_2H_7SSn]^+$, 166.95 $[C_2H_7OSn]^+$, 150.9 $[C_2H_7Sn]^+$

Sample **1a**, (+)TOF MS: *m/z* 384.10 $[C_{13}H_{30}NO_2SSn]^+$, 639.04 $[C_{18}H_{40}NO_4S_2Sn_2]^+$, 619.26 $[C_{18}H_{38}NO_3S_2Sn_2]^+$.

Sample **2a**, (+)TOF MS: *m/z* 428.09 $[C_{14}H_{30}NO_4SSn]^+$, 726.02 $[C_{20}H_{40}NO_8S_2Sn_2]^+$, 707.01 $[C_{20}H_{38}NO_7S_2Sn_2]^+$, 619.89 $[C_{12}H_{21}O_8NaS_2Sn_2]^+$.

Sample **3a**, (+)TOF MS: *m/z* 384.10 $[C_{13}H_{30}NO_2SSn]^+$, 639.04 $[C_{18}H_{40}NO_4S_2Sn_2]^+$, 619.26 $[C_{18}H_{38}NO_3S_2Sn_2]^+$.

Sample **1b**, (−)TOF MS: *m/z* 358.94 $[C_8H_{15}O_4S_2Sn]^-$, 312.9389 $[C_7H_{13}O_2S_2Sn]^-$, 288.94 $[C_5H_{13}O_4SSn]^-$.

Sample **2b**, (−)TOF MS: *m/z* 296.92 $[C_6H_9O_4SSn]^-$, 446.92 $[C_{10}H_{15}O_8S_2Sn]^-$

Sample **3b**, (−)TOF MS: *m/z* 358.94, $[C_8H_{15}O_4S_2Sn]^-$, 312.94 $[C_7H_{13}O_2S_2Sn]^-$, 288.94 $[C_5H_{13}O_4SSn]^-$.

A representative ESI MS spectrum of sample **1a** is shown in Fig. 1.

NMR equipment and procedure

^{1}H NMR measurements in solution were performed by means of a Bruker AMX R-300 spectrometer. The chemical shifts were measured with respect to 1,4-dioxane, which was used as internal reference, and converted relative to TMS using $\delta_{dioxane}$ = 3.70 ppm. Investigations were carried out in a 9 : 1 H_2O–D_2O mixture. The concentrations of dimethyltin(IV) cation and ligands were varied in the range 5–10 mmol L^{-1}. In order to calculate the individual NMR parameters (δ, ^2J) of the formed species, the spectra were recorded at various pH between 2 and 10. The individual NMR parameters belonging to the hydrolysed species of dimethyltin(IV) and to the dimethyltin(IV)–ligand complexes were calculated assuming fast mutual exchange.[37] The heteronuclear couplings relative to tin-bound methyl groups $^2J(^{119}Sn–^1H)$ determined in such a way were converted into C–Sn–C angles according to the published equations.[38]

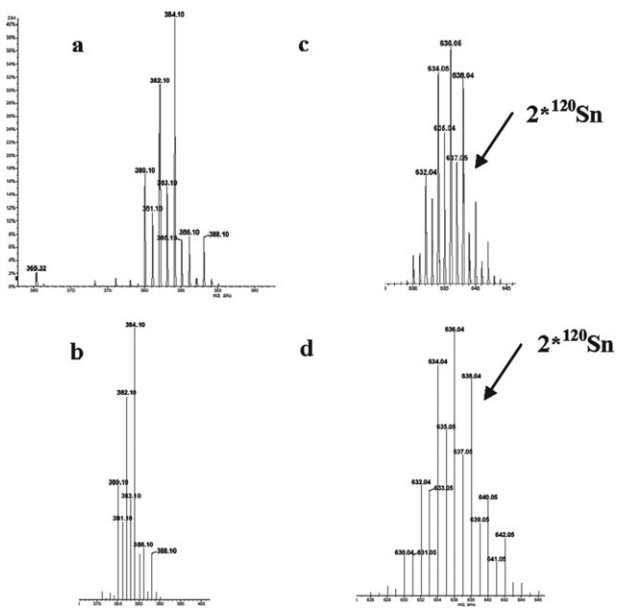

Fig. 1 ESI MS spectrum of sample **1a**. Observed (a, c) and theoretical (b, d) isotopic abundances of ions containing one and two tin atoms. The most abundant natural isotope is ^{120}Sn.

Calculations

The following computer programs were used: (i) BSTAC and STACO to refine all the parameters of an acid–base titration (such as analytical concentration of reagent and E^0) and to calculate complex formation constants; (ii) ES4ECI to draw distribution diagrams and to calculate the formation percentage of each species.[39] Small variations of I in the different titrations can be taken into account by the programs BSTAC and STACO. For the dependence of formation constants on ionic strength, the Debye–Hückel type equation is used:[40]

$$\log\beta = \log {}^{T}\beta - 0.51z^*\sqrt{I}/(1 + 1.5\sqrt{I}) + CI + DI^{3/2} \quad (1)$$

$p^* = \sum p_{reactants} - \sum p_{products}$; $z^* = \sum z^2_{reactants} - \sum z^2_{products}$, β = formation constant; $^T\beta$ = formation constant at zero ionic strength; p and z are stoichiometric coefficients and charges, respectively. The value of empirical parameter C was chosen on the basis of previous experimental data on the dependence on ionic strength for similar systems.

All the formation data were corrected to I = 0.01 mol L^{-1}; at I < 0.05 mol L^{-1}, $\sigma(\log\beta) \sim 0.15I$, and therefore, since the ionic strength in our measurements was always less than 0.020 mol L^{-1}, the contribution of this extrapolation procedure to the total error is less than 0.003.

Since alkyltin cations show a strong tendency to hydrolysis, hydroxo species formed by dimethyltin(IV) cation must be considered when studying interactions with ligands. The weak interactions of dimethyltin(IV) with small amounts of Cl^- from the dimethyltin(IV) chlorides were also taken into account in the calculations. The hydrolysis constants of dimethyltin(IV) have already been reported.[26] Equilibrium constants for hydrolysis and Cl^- complexes of dimethyltin(IV) cation are reported in Table 1. These constants are affected by fairly low errors (±0.05 log units, for mononuclear species, and ~0.1 log units for polynuclear and chloride species) and, therefore, are suitable for the characterization of speciation schemes. Analogously, the protonation of the mercaptocarboxylate ligands under investigation must be taken into account; they were also determined in this work and are shown in Table 2.

Table 1 Equilibrium constants[a] for hydrolysis and Cl^- complexes of dimethyltin(IV) at $I = 0.01$ mol L^{-1} and $T = 25$ °C

p q r	$\log \beta_{pqr}{}^{a}$ $(CH_3)_2Sn^{2+}$ [b]
1 −1 0	−2.94
1 −2 0	−8.24
1 −3 0	−19.35
2 −2 0	−5.07
2 −3 0	−9.23
1 0 1	0.61
1 −1 1	−3.33

[a] β_{pqr} refer to the reaction: $pM^{2+} + qH_2O + rCl^- \leftrightarrows M_p(OH)_qCl_r^{2p+q-r} + qH^+$. [b] Calculated from data at $I = 0$ mol L^{-1} from ref. 26 and 31.

Table 2 Protonation constants of mercaptocarboxylates and formation constants of $(CH_3)_2Sn$–mercaptocarboxylate species at $T = 25$ °C and $I = 0.01$ mol L^{-1}

	$\log \beta_{pqr}{}^{a}$		
p q r	L = TLA	L = MPA	L = TMA
0 1 1	10.13 ± 0.01[b]	10.29 ± 0.01[b]	10.54 ± 0.01[b]
0 1 2	13.96 ± 0.01	14.28 ± 0.02	15.25 ± 0.01
0 1 3	—	—	18.32 ± 0.02
1 1 0	12.65 ± 0.05	11.72 ± 0.05	13.45 ± 0.05
1 1 1	14.4 ± 0.1	14.9 ± 0.2	17.70 ± 0.10
1 1 −1	5.94 ± 0.08	4.81 ± 0.05	6.40 ± 0.05
2 1 0	—	—	17.05 ± 0.15
1 2 0	18.88 ± 0.07	—	18.97 ± 0.15
1 2 2	—	28.93 ± 0.10	—

[a] Reaction: $pM^{2+} + qL^{z-} + rH_2O \leftrightarrows M_pL_q(OH)_r^{(2-z-r)} + rH^+$. [b] $\pm 3\sigma$ (σ = standard deviation).

Results and discussion

Complexes of dimethyltin(IV) with mercaptocarboxylates and speciation profiles

Complex formation constants of dimethyltin(IV) (M) with mercaptocarboxylates (L) are expressed as $\log \beta_{pqr}$, according to the equilibrium reaction:

$$pM^{2+} + qL^{z-} + rH_2O \leftrightarrows M_pL_q(OH)_r^{(2-z-r)} + rH^+ \quad (2)$$

The formation constant values of dimethyltin(IV)–mercaptocarboxylate species, calculated at $I = 0.01$ mol L^{-1} by means of eqn (1) are reported in Table 2 together with errors given as standard deviations. As can be seen the stability of these species is high, in particular for TMA, so that speciation profiles with high formation percentages of complex species in a wide pH range can be expected. Fig. 2–4 show the speciation diagrams of $(CH_3)_2Sn^{2+}$–TLA, $(CH_3)_2Sn^{2+}$–MPA and $(CH_3)_2Sn^{2+}$–TMA systems, respectively, at two different M : L concentration ratios: M : L = 1 : 2 with $C_M = 5$ mmol L^{-1} (a) and M : L = 1 : 1 with $C_M = 1$ mmol L^{-1} (b).

The speciation diagrams of dimethyltin(IV)–TLA system at different concentration ratios show that: (1) in the acid pH range, both at M : L = 1 : 2 (Fig. 2(a)) and at M : L = 1 : 1 (Fig. 2(b)), the most important species is ML^0, with formation over 80% at $3.5 \leq$ pH ≤ 5.5; while MLH^+ is present in significantly lower amount; (2) in the alkaline pH range, at M : L = 1 : 2 (Fig. 2(a)), the highest yield is achieved by

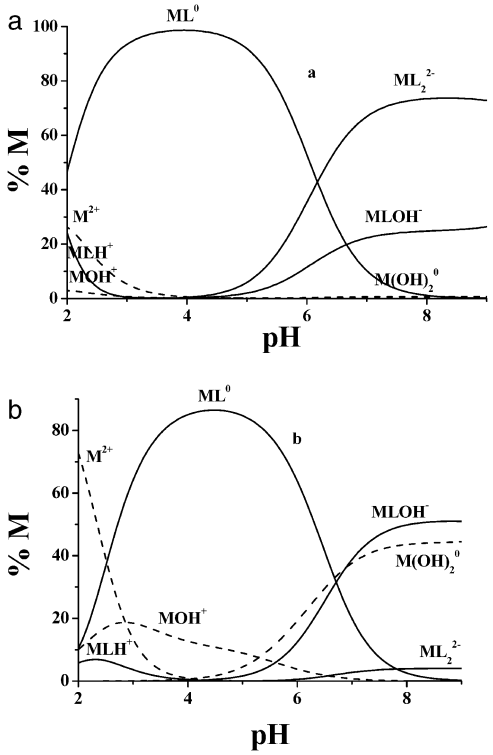

Fig. 2 Speciation diagrams of dimethyltin(IV)–TLA (M–L) *vs.* pH at $T = 25$ °C, without supporting electrolyte. Indexes refer to reaction (2). Free metal and hydrolytic species are shown by dashed lines: (a) $C_M = 5$ mmol L^{-1}; $C_L = 10$ mmol L^{-1}; (b) $C_M = C_L = 1$ mmol L^{-1}.

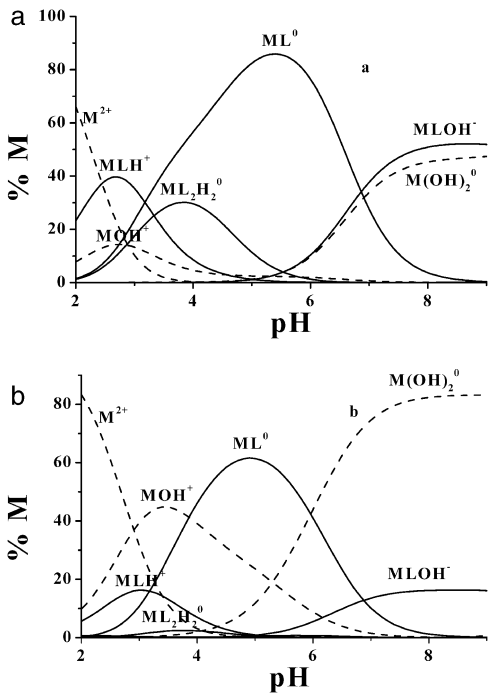

Fig. 3 Speciation diagrams of dimethyltin(IV)–MPA (M–L) *vs.* pH at $T = 25$ °C, without supporting electrolyte. Indexes refer to reaction (2). Free metal and hydrolytic species are shown by dashed lines: (a) $C_M = 5$ mmol L^{-1}; $C_L = 10$ mmol L^{-1}; (b) $C_M = C_L = 1$ mmol L^{-1}.

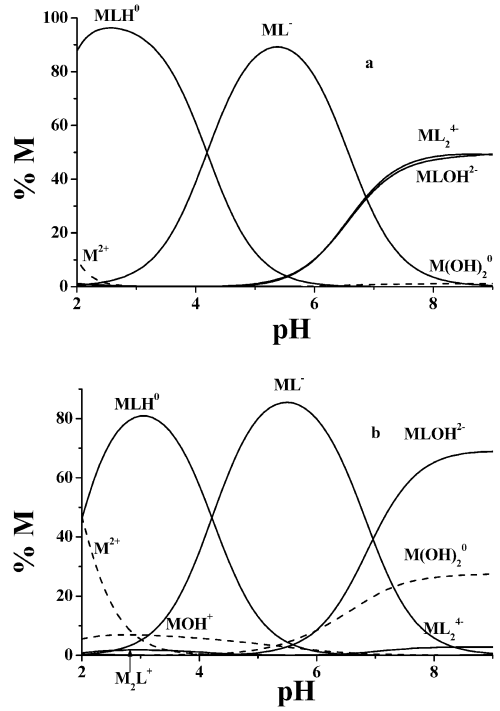

Fig. 4 Speciation diagrams of dimethyltin(IV)–TMA (M–L) *vs.* pH at T = 25 °C, without supporting electrolyte. Indexes refer to reaction (2). Free metal and hydrolytic species are shown by dashed lines: (a) C_M = 5 mmol L^{-1}; C_L = 10 mmol L^{-1}; (b) $C_M = C_L$ = 1 mmol L^{-1}.

ML_2^{2-} (≈70% at pH = 8) while a lower formation of $MLOH^-$ species (≈20% at pH = 8) can be observed; at M : L = 1 : 1 (Fig. 2(b)) and at lower ligand concentration (C_L = 1 mmol L^{-1}), the most important complex species $MLOH^-$ (≈50% at pH = 8) prevails over $M(OH)_2^0$ hydrolytic species (≈40% at pH = 8).

In the dimethyltin(IV)–MPA system: (1) at M : L = 1 : 2 (Fig. 3(a)), in the acid pH range, MLH^+ and ML^0 are present, together with the $ML_2H_2^0$ species (30% at pH = 4); in the alkaline pH range, $MLOH^-$ and the hydrolytic $M(OH)_2^0$ species are the most relevant (about 45 and 50%, respectively, at pH = 8); (2) at M : L = 1 : 1 (Fig. 3(b)), ML^0 species remains relevant (over 60% at pH = 5) and at alkaline pH values the hydrolytic $M(OH)_2^0$ species prevails on all.

Speciation diagrams of dimethyltin(IV)–TMA systems at different concentration ratios show no significant difference in the acid pH range; on the contrary, in the alkaline pH range, at M : L = 1 : 2 (Fig. 4(a)), $MLOH^{2-}$ and ML_2^{4-} are the most important species with formation of about 50% for both, at pH = 8; at M : L = 1 : 1 (Fig. 4(b)), $MLOH^{2-}$ species reaches about 70% at pH = 8, while ML_2^{4-} is negligible. It must be noted that even at $C_M = C_L$ = 1 mmol L^{-1}, for TLA and especially for TMA containing systems, in the $7 \leq pH \leq 8.5$ range, of interest for natural waters, the formation of MLOH species reduces the hydrolysis of dimethyltin(IV) cation; while in the case of MPA containing systems, in the same conditions, the simple hydrolytic species $M(OH)_2^0$ reaches very high formation percentages.

Sequestering ability of mercaptocarboxylates towards dimethyltin(IV)

The sequestering ability of a ligand towards a metal can be expressed by the function $\sum(\%)$ *vs.* pL, where $\sum(\%)$ is the total percentage of dimethyltin(IV) complexed and $pL = -\log[L]_{tot}$. Since this function is a typically sigmoidal curve (or a dose response curve), increasing rapidly over a relatively low change in concentration, we can use the Boltzmann type equation (with asymptotes of 100 for $pL \rightarrow -\infty$ and 0 for $pL \rightarrow +\infty$):

$$\Sigma(\%) = 100 \times \left[\frac{1}{1 + e^{(pL - pL_{50})/S)}} - 1\right] \qquad (3)$$

where pL_{50} is an empirical parameter, which defines the ligand concentration necessary to sequester 50% of cation and S is a measure of the slope in flex of the function ($\sum\%$) *vs.* pL. The pL_{50} parameter is very useful because it gives a representation of the binding ability of a ligand (L) toward a specific cation in the investigated conditions.[34,35]

Fig. 5 shows the sequestering power of TLA and TMA toward dimethyltin(IV) at C_M = trace, pH = 7.4, T = 25 °C, without supporting electrolyte. These two different mercaptocarboxylates have a very similar ability to sequester dimethyltin(IV) cation, in these conditions pL_{50} values are: 4.08, 4.18, for TLA and TMA, respectively. The sequestering ability of MPA is lower: pL_{50} = 2.49 (S = −1 in all cases). The three mercaptocarboxylates under study show a good sequestering ability towards dimethyltin(IV), especially if compared to that of bi- or tri-carboxylates, such as malonate (mal) or 1,2,3-propanetricarboxylate (tca); for example at pH = 5, pL_{50} = 3.73, 5.18, 5.47, for MPA, TLA and TMA respectively, while pL_{50} = 2.48, 2.77 for mal and tca, respectively.[34]

Mass spectra results

Solutions prepared from simply mixing of dimethyltin(IV) and ligand are analyzed by ESI-MS in both polarity modes to obtain complementary structure information *in situ* of the major product. MS/MS experiments were performed to elucidate the ionic structure and also to characterize fragmentation patterns. The characteristic natural isotopic pattern for tin atoms having ten isotopes, where ^{120}Sn is the most abundant,

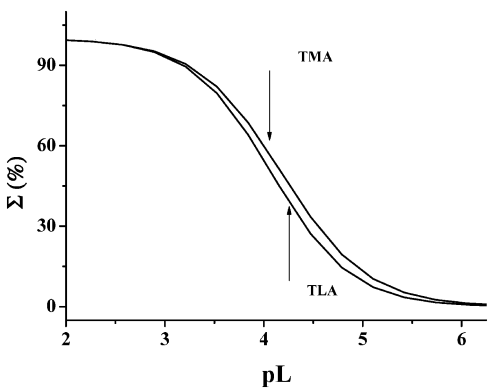

Fig. 5 Sum of percentages of dimethyltin(IV)–TLA, and dimethyltin(IV)–TMA species *vs.* pL at C_M = trace, pH = 7.4, T = 25 °C, without supporting electrolyte.

was an important tool in the interpretation of mass spectra of organotin compounds, especially for the proton bound dimeric species generated under the adopted experimental conditions. The elemental composition of all compounds is verified by the comparison of the measured experimental isotopic distribution with the theoretically calculated distribution of the expected summary formula.

Direct mass spectrometric measurements of solutions containing both tin species and ligand are quite difficult, even under the softest ionization conditions. The corresponding ions related to ML or ML_2 species are often missing completely in the full-scan spectra of corresponding solution. To overcome this difficulty, samples were prepared in different conditions of pH and M : L ratios. Our identification approach is demonstrated on the example of sample **3**. The pH of the aqueous solution of samples **1–3**, containing both $(CH_3)_2SnCl_2$ and ligand with a final M : L ratio of 1 : 10, is *ca.* 2.2; in this condition a clear solution was observed.

The ion-providing information on M : L species was observed in the full-scan positive ion ESI mass spectra by direct infusion of samples **1–3**. In accordance with the speciation diagrams of MPA (Fig. 2(a)), which shows that at pH = 2.2 the main complex species in solution is MLH^+, the positive ion spectrum of sample **3** reveals the species $[ML + H]^+$ at m/z 254.95 and the corresponding dimeric adduct $[ML–H–ML]^+$ at m/z 508.89 (m/z values are related to the ^{120}Sn isotope); fragment ions are missing. Fig. 6(a)–(d) illustrate a good correlation between the theoretically calculated and experimentally measured isotopic abundances of $[ML + H]^+$ ($[C_5H_{11}O_2SSn]^+$) and $[ML–H–ML]^+$ ($[C_{10}H_{21}O_4S_2Sn_2]^+$) ions. This correlation was used as supporting information for the suggestion of the composition of the individual ions, which is useful mainly for "*in situ*" generated complexes containing one or more tin atoms and for hydrolysis products. These results clearly indicate that both chloride anions dissociate from dimethyltin dichloride and that under the adopted experimental condition solvent does not compete towards cation.

The use of ligands having multiple donor sites led to intramolecular stabilization of several highly reactive compounds[41] and organotin cations.[42,43] Moreover, it is known that carboxylic acids bearing donor groups in their α or β positions act as bidentate ligands, giving rise to cyclic structures.[44] Accordingly, the formation of $[ML + H]^+$ species suggests that MPA acts as bidentate ligand giving rise to structure **3** (Fig. 7).

Analogously, TLA leads to the cyclic structure **1** (Fig. 7). The proposed complex structures of $[ML + H]^+$ observed in spectra of **1–3** are confirmed by MS/MS analysis. In MS/MS analyses, many characteristic fragment ions can be found and correlate with the structure. In particular, for all species the MS/MS spectrum reveals the characteristic neutral losses corresponding to the functional groups, such as H_2O ($\Delta m/z$ 18 Da), carbon dioxide ($\Delta m/z$ 44 Da) and formic acid ($\Delta m/z$ 46 Da), typical for the carboxylic group.

MS/MS of the precursor $[ML + H]^+$ (m/z 254.95, sample **3**) yields a fragment rich product mass spectrum (Fig. 8); the neutral logical losses are found such as $[MLH - H_2O]^+$ ($[C_5H_9OSSn]^+$) at m/z 236.9, $[MLH - CH_2O_2]^+$ ($[C_4H_9SSn]^+$) at m/z 208.9 and $[MLH - C_3H_4O_2]^+$ ($[C_2H_7SSn]^+$) at m/z 182.9 while the ion species at m/z 166.9 can be attributed to a formation of $[C_2H_7OSn]^+$ cation. These results confirm O→Sn and S→Sn coordination and the hypothesized cyclic structures. The complete fragmentation pattern of the $[ML + H]^+$ ion (m/z 254.95, $[C_5H_{11}O_2SSn]^+$) (Fig. 9) is proposed on the basis of interpretation of its MS/MS spectrum. Similar fragmentation patterns are proposed for sample **1**.

A five-membered cyclic structure is proposed for sample **2** (Fig. 7) on the basis of observed consecutive and/or direct neutral losses. In particular, the formation of the ion species at m/z 239.9, can be generated preferentially from a

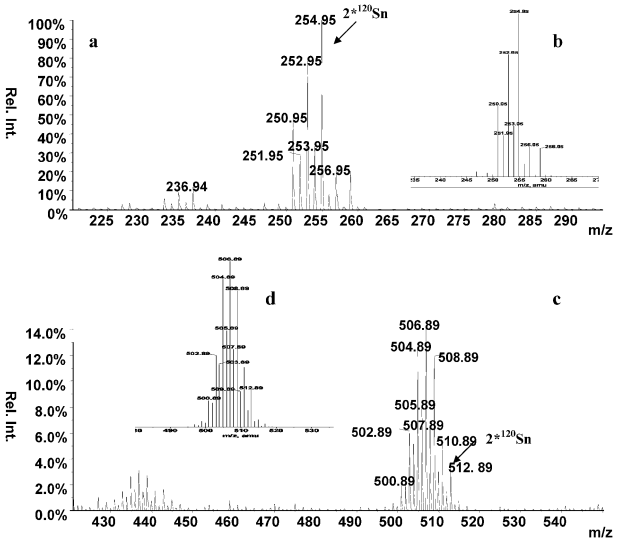

Fig. 6 Positive ion spectrum of sample **3**. Observed (a, c) and theoretical isotopic abundances (b, d) of ions containing one and two tin atoms. The most abundant natural isotope is ^{120}Sn.

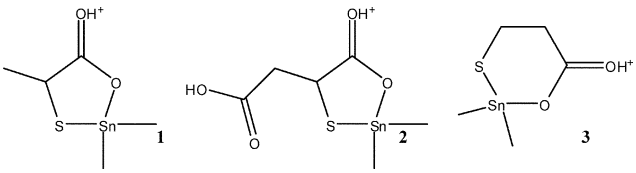

Fig. 7 Proposed structures for samples **1–3**.

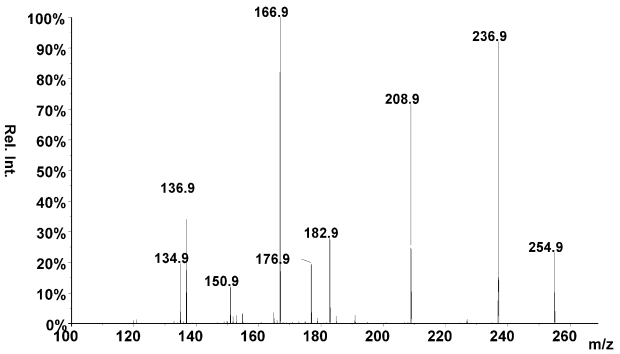

Fig. 8 MS/MS spectrum of $[ML + H]^+$ (m/z 254.95) obtained from sample **3**.

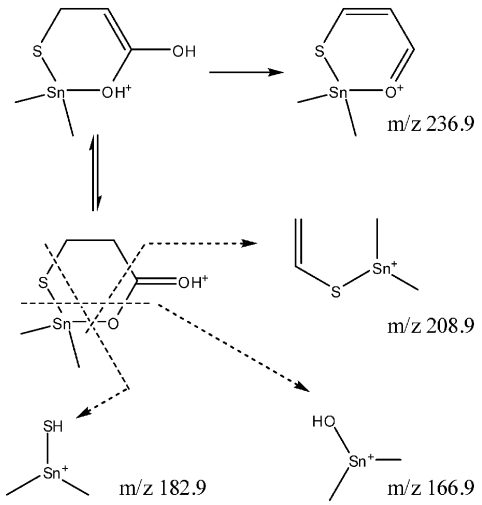

Fig. 9 Fragmentation pathway of sample **3**.

five-membered structure by the direct release of one formal unit of acetic acid (Fig. 10).

The corresponding ions related to the ML_2 species were missing completely in the full-scan positive spectra of solutions **1–3**. The ESI MS profiles resulting from samples **1–3** match those obtained by speciation models (Fig. 2–4). The obvious difference between the two methods is represented by the specificity of the mass spectrometric method, which allows structure information of the M : L pool through the determination of the molecular weight of each species. The pH of the solution containing the ligand was raised to 9.0, in order to observe other possible complex species. This was performed using DIPEA, a good organic base characterized by high solubility in aqueous medium. Addition of a few μL of DIPEA (1.5 mmol L^{-1}) to an aqueous solution of dimethyltin(IV)–ligand (M–L) with a final M : L ratio of 1 : 10 (samples **1a–3a**), followed by running the positive ion spectrum yielded $[ML + C_8H_{20}N]^+$ and $[ML + C_8H_{20}N + ML]$ adducts. The major peak was due to the $[ML + C_8H_{20}N]^+$ adduct at m/z 384.10 accompanied by a dimeric form $[ML + C_8H_{20}N + ML]^+$ in decreasing order of intensity, as when DIPEA was not added (pH = 2.2, samples **1–3**). The presence of the tertiary organic amine improves the signal-to-noise ratio and the precision of the comparison of experimental isotopic distributions with the theoretical ones (Fig. 1, see Experimental section).

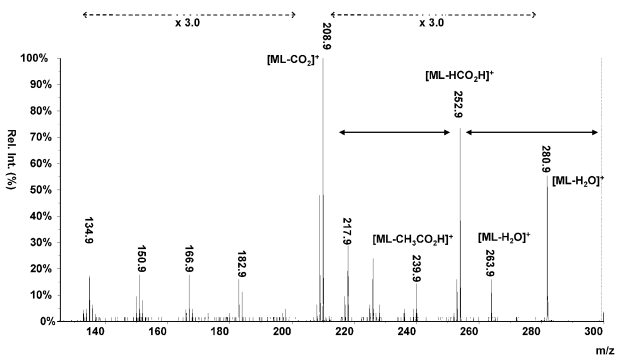

Fig. 10 ESI MS/MS of sample **2**.

The formation of the $[ML + C_8H_{20}N]^+$ adduct in the full-scan positive ion ESI confirms that all studied mercaptocarboxylic acids act as bidentate ligands, in accordance with the suggested structures (Fig. 7).

Contrary to the positive ion mode, the ion providing information on ML species was observed only in the full-scan negative ion ESI mass spectrum by direct infusion of sample **2b**. The formation of $[ML - H]^-$ at m/z 296.92, (Δppm = −6.4 is accompanied by very low abundant ions $[ML_2 - H]^-$ at m/z 446.92). The good correlation between the theoretically calculated and experimentally measured isotopic abundances of $[ML - H]^-$ species ($[C_6H_9O_4SSn]^-$, m/z 296.92) clearly indicates that upon adopted experimental conditions the formation of cyclic structure is preferred for sample **2b**.

On the contrary, for samples **1b** and **3b** the base peak of their full-scan negative ion spectra is the ion species $[ML(OH) + H_2O - H]^-$ accompanied by the less abundant $[ML_2 - H]^-$ and $[ML_2 - H - HCOOH]^-$ (Fig. 11). These results are in accordance with the speciation diagrams of TLA and MPA (Fig. 2 and 3), which show the formation of the $MLOH^-$ complex species. The formation of the solvated species $[ML(OH) + H_2O - H]^-$ (m/z 288.94, $[C_5H_{13}O_2S_2Sn]^+$) is in agreement with the adopted experimental condition.

NMR measurements

In order to obtain further information about the species formed by dimethyltin(IV) with the ligands under study, as well as on their structure, ^1H NMR spectra in H_2O–D_2O solution were carried out. We choose two of the three mercaptocarboxylates: TLA as acid having one carboxylic and one sulfidrilic group, and TMA, having one carboxylic and two sulfidrilic groups.

Concerning the tin-bound CH_3 signals, independently from the metal : ligand ratio employed, the NMR spectra of dimethyltin(IV), as well as of both dimethyltin(IV)–TMA and dimethyltin(IV)–TLA solutions, show a single sharp signal together with the satellite peaks of heteronuclear couplings with the two NMR active isotopes of tin namely $^2J(^{119}Sn–^1H)$ and $^2J(^{117}Sn–^1H)$, as observed for similar systems already investigated.[32,35] In the spectra of pure dimethyltin(IV) the chemical shift of methyl protons decrease steadily by increasing pH, whilst for the tin-bound CH_3 resonances detected in the

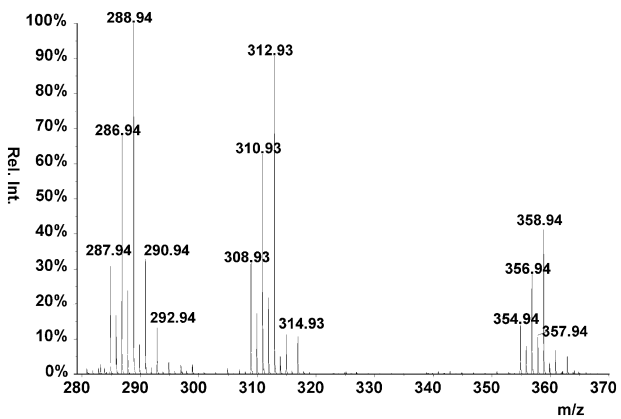

Fig. 11 ESI(−) spectrum of sample **1b**.

ligand containing solutions the observed decrease is less dramatic up to pH = 4.5.

The lines depicted in Fig. 12(a) and (b), representing the variations of δ_{SnCH_3} *vs.* pH for the two studied systems, clearly show that, regardless of the coincidence at about pH 4.3 and 7, these CH_3 protons are shifted upon the presence of ligands. This spectral evidence indicates the involvement of the metal not only in hydrolysis but also in other interactions clearly due to the presence of coordinating groups in solution. It is worth mentioning that for dimethyltin(IV)–TLA spectra the TLA methyl resonance is much less affected by the tin presence than the CH group suggesting that methyne is more influenced by the coordination occurring upon pH variation. By comparing the spectra of the dimethyltin(IV)–TLA system recorded at 1 : 1 and 0.5 : 1 ratios, respectively, at low pH, it appears that all the shifts are quite similar; however, the signals are broader for 1 : 1 ratio. For dimethyltin(IV) : TLA = 0.5 : 1, at pH 3.6, two peaks, attributable to CH for bound and free TLA (3.77 and 3.51 ppm, respectively), can be observed; furthermore, the bound CH signal can be confidently assigned to ML complex, as suggested by the spectrum registered at the same pH for the 1 : 1 solution as well as by the potentiometric studies. This downfield shift of CH resonance can be ascribed to the coordination of the deprotonated SH group to tin as suggested by Gajda-Schrantz *et al.* for analogous diethyltin(IV) complexes.[19] By increasing the pH, the tin-bound CH_3 signal appears as a single resonance with comparable chemical shift despite the stoichiometric ratio employed. On the contrary the TLA methyl resonance of the 0.5 : 1 solutions appears at an intermediate chemical shift between those shown in the pure TLA and in the metal–ligand 1 : 1 system.

Concerning TMA containing solutions, the trends showed by the CH signal due to coordination upon pH variation is analogous, even though TMA is featured by the presence of an additional coordinating site with respect to TLA. Looking at the spectra of the dimethyltin(IV)–TMA system recorded at 1 : 1 ratio, the peak due to the methyne group can be observed as a single resonance at δ values rather higher than those detected in the experiments carried out on pure TMA solutions, for a given pH. At the same time, for dimethyltin(IV)–TMA spectra recorded employing 0.5 : 1 ratio, CH signals appear hardly detectable up to pH $\approx$ 5 whereas at higher pH two peaks clearly due to the methyne group for bound and free TMA can be distinguished (at 3.95 and 3.56 ppm, respectively). By increasing pH these two resonances are upfield shifted, as for the other signals.

For pure TMA solutions only a single resonance is observed for the methylene group, regardless of the pH, meaning that all the species are involved in a fast exchange. In the case of dimethyltin(IV)–TMA 1 : 1 solutions, the shift of the signal due to the CH_2 group is only slightly affected by the presence of the metal in the acidic pH range as shown by the slight line slope; again, only a single signal is observable. Whenever the NMR solution experiments are carried out in a twofold excess of TMA with respect to dimethyltin(IV), the CH_2 pattern is different from the already discussed signals. Regardless of the chemical shift, that is comparable to the dimethyltin(IV)–TMA 1 : 1 spectra at the same pH, the signals appear broader suggesting that the bound and free TMA slowly exchange on the NMR time scale. Unfortunately no other information can be confidently obtained from these peaks.

As already discussed, the tin-bound methyl groups appear as a single resonance in all the experimental conditions employed to perform the various spectra, both for TLA and TMA systems; in these conditions the individual NMR parameters of the formed complexes cannot be rationalized directly from the spectra. Nevertheless, by using the speciation data it is possible to calculate the individual chemical shifts as well as coupling constants since the concentration of each complex at different pHs is known. As a consequence, the individual δ and J values can be used to recalculate the corresponding mean values at a given pH so that the observed and calculated mean NMR parameters can be compared in order to validate the model employed for the calculation of each complex formed as well as to confirm the model used for the rationalization of potentiometric data. Fig. 13 shows the excellent agreement between calculated and observed chemical shifts, both for TLA- and TMA-containing systems, thus confirming the model proposed in the potentiometric study.

In addition, the calculated J for each complex species can be converted into a C–Sn–C angle by means of the published equation by Lockhart and Manders[38] in order to obtain qualitative information about the geometry of the complexes around the tin. For the dimethyltin(IV)–TLA complexes, all the ^2J such obtained range between 73.3 and 76.8 Hz (see Table 3), corresponding to angles matching with a Tbp arrangement around the metal while in the case of dimethyltin(IV)–TMA the complexes ML^- and MLH^0 are also featured by ^2J corresponding to a Tbp geometry, while the values obtained for ML_2^{4-} and $MLOH^{2-}$ suggest a tetrahedral and octahedral arrangement around the tin, respectively.

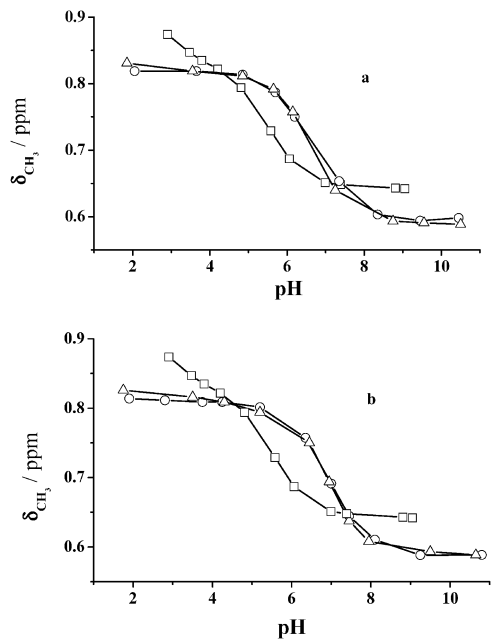

Fig. 12 Measured chemical shifts of $SnCH_3$ *vs.* pH for TLA (a) and TMA (b): (□) solutions containing dimethyltin(IV) only; (○) dimethyltin(IV) : ligand = 1 : 2 mixtures; (△) dimethyltin(IV) : ligand = 1 : 1 mixtures.

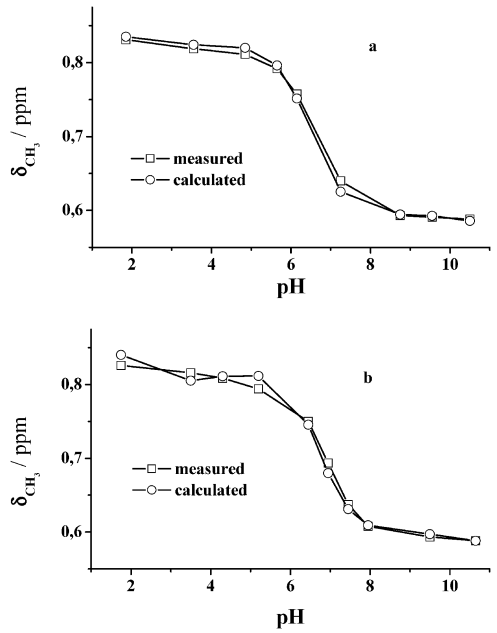

Fig. 13 Chemical shifts of CH_3 *vs.* pH in dimethyltin(IV)–L 1 : 1 mixtures: (a) L = TLA, (b) L = TMA.

Conclusions

The stability of dimethyltin(IV)-mercaptocarboxylate species is high, in particular for TMA; speciation profiles show high formation percentages of complex species in a wide pH range. Sequestering ability towards dimethyltin(IV) cation is good, mainly for TMA and TLA, even at physiological pH and is markedly higher than that of di- and tri-carboxylic ligands.

ESI experiments confirm the presence and the stoichiometry of dimethyltin(IV)–mercaptocarboxylate species and also allow elucidation of their structures. Full scan positive ion spectra show $[ML + H]^+$ species for all the three mercaptocarboxylates investigated. Moreover MS/MS analysis confirms the proposed cyclic structures with O→Sn and S→Sn coordination (Fig. 7). The formation of $[ML + C_8H_{20}N]^+$ adducts, in presence of DIPEA, confirms that all these mercaptocarboxylates studied act as bidentate ligands, in accordance with the suggested structures. Information about $[ML - H]^-$ or solvated species $[ML(OH) + H_2O - H]^-$ was obtained in full scan negative ion spectra.

Table 3 Calculated individual ^{1}H NMR parameters for dimethyltin(IV)–thiolactate and –thiomalate species

Ligand	Species	$\delta(CH_3)$/ppm	^2J(Sn–H)/Hz	∠C–Sn–C/°
TLA	ML	0.827 ± 0.005[a]	78	129
	MLH	0.72 ± 0.03		—
	MLOH	0.562 ± 0.009	73	123
	ML_2	0.66 ± 0.02	77	130
TMA	ML	0.821 ± 0.007	76	126
	MLH	0.805 ± 0.003	85	138
	MLOH	0.581 ± 0.006	95	153
	ML_2	0.7 ± 0.2	57	111

[a] ±Standard deviation.

^{1}H NMR measurements show an excellent agreement between calculated and observed chemical shifts (see Fig. 13) both for TLA- and TMA-containing systems, confirming the speciation model proposed by the potentiometric study. In addition, for dimethyltin(IV)–TLA complexes, the ^2J values obtained, for ML^0, $MLOH^-$ and ML_2^{2-} species, correspond to angles matching with a Tbp arrangement around the metal; in the case of dimethyltin(IV)–TMA the complexes ML^- and MLH^0 are also featured by ^2J corresponding to Tbp geometry, while the values obtained for ML_2^{4-} and $MLOH^{2-}$ suggest a tetrahedral and octahedral arrangement around the tin, respectively.

Acknowledgements

This work was supported by grants from the University of Messina (PRA) and the University of Calabria.

References

1 S. J. Blunden, P. A. Cusack and R. Hill, *The Industrial Use of Tin Chemicals*, Royal Society of Chemistry, London, 1985.
2 M. A. Champ and P. P. Seligman, Organotin Compounds in the Environment, in *Organometallic Compounds in the Environment*, ed. P. J. Craig, Longman, Harlow, Essex, UK, 1986, pp. 111–159.
3 R. Frache and P. Rivaro, in *Occurence, Pathways and Bioaccumulation of Organometallic Compounds in Marine Environments*, ed. A. Gianguzza, E. Pellizzetti and S. Sammartano, Springer-Verlag, Berlin, Heidelberg, 2000, pp. 201–211.
4 C. Huey, F. E. Brinkman, S. Grim and W. P. Iverson, in *Proc. Int. Conf. Transport of Persistent Chemicals in Aquatic Ecosystems*, National Research Council Canada, Ottawa, 1974, pp. 73–78.
5 P. H. Quevauviller and O. F. X. Donard, Tin speciation monitoring in estuarine and coastal environments, in *Element Speciation in Bioinorganic Chemistry*, ed. S. Caroli, John Wiley & Sons, New York, 1996, pp. 331–362.
6 H. E. Guard, A. B. Cobet and W. M. Coleman, *Science*, 1981, **213**, 770–771.
7 L. E. Hallas, J. C. Means and J. J. Cooney, *Science*, 1982, **215**, 1505–1507.
8 R. J. Maguire and R. J. Tkacz, *J. Agric. Food Chem.*, 1985, **33**, 947–953.
9 J. H. Weber and J. J. Alberts, *Environ. Technol.*, 1990, **11**, 3–8.
10 S. Chiavarini, C. Cremisini and R. Morabito, Organotin compounds in marine organisms, in *Element Speciation in Bioinorganic Chemistry*, ed. S. Caroli, John Wiley & Sons, New York, 1996, pp. 287–329.
11 M. Nath, S. Pokharia and R. Yadav, *Coord. Chem. Rev.*, 2001, **215**, 99–149.
12 H. Jankovics, L. Nagy, Z. Kele, C. Pettinari, P. D'Agati, C. Mansueto, C. Pellerito and L. Pellerito, *J. Organomet. Chem.*, 2003, **668**, 129–139.
13 M. Gielen, *Coord. Chem. Rev.*, 1996, **151**, 41–51.
14 L. Pellerito and L. Nagy, *Coord. Chem. Rev.*, 2002, **224**, 111–150.
15 M. M. Shoukry, *Talanta*, 1996, **43**, 177–183.
16 A. Silvestri, D. Duca and F. Huber, *Appl. Organomet. Chem.*, 1988, **2**, 417–425.
17 N. Buzás, T. Gajda, E. Kuzmann, L. Nagy, A. Vértes and K. Burger, *Main Group Met. Chem.*, 1995, **18**, 641–649.
18 G. Berthon, *Pure Appl. Chem.*, 1995, **67**, 1117–1240.
19 K. Gajda-Schrantz, L. Nagy, T. Fiore, L. Pellerito and T. Gajda, *J. Chem. Soc., Dalton Trans.*, 2002, 152–158.
20 D. Dakternieks, H. Zhu, E. R. T. Tiekink and R. Colton, *J. Organomet. Chem.*, 1994, **476**, 33–40.
21 M. Biesemans, A. Duthie, K. Jurkschat, I. Verbruggen, R. Willem and Z. B., *Appl. Organomet. Chem.*, 2003, **17**, 298–304.
22 R. Colton, A. D'Agostino and J. C. Traeger, *Mass Spectrom. Rev.*, 1995, **14**, 79–106.
23 E. Rosenberg, *J. Chromatogr., A*, 2003, **1000**, 841–889.

24 K. Lemr, M. Holčapek, P. Jandera and A. Lyčka, *Rapid Commun. Mass Spectrom.*, 2000, **14**, 1881–1888.
25 K. W. M. Siu, G. J. Gardner and S. S. Berman, *Anal. Chem.*, 1989, **61**, 2320–2322.
26 C. De Stefano, C. Foti, A. Gianguzza, M. Martino, L. Pellerito and S. Sammartano, *J. Chem. Eng. Data*, 1996, **41**, 511–515.
27 C. De Stefano, C. Foti, A. Gianguzza, F. Marrone and S. Sammartano, *Appl. Organomet. Chem.*, 1999, **13**, 805–811.
28 C. De Stefano, C. Foti, A. Gianguzza, F. J. Millero and S. Sammartano, *J. Solution Chem.*, 1999, **28**, 959–972.
29 C. Foti, A. Gianguzza, F. J. Millero and S. Sammartano, *Aquatic Geochem.*, 1999, **5**, 381–398.
30 C. De Stefano, C. Foti, A. Gianguzza and S. Sammartano, Hydrolysis processes of organotin(IV) compounds in sea water, in *Chemical Processes in Marine Environments*, ed. A. Gianguzza, E. Pelizzetti and S. Sammartano, Springer-Verlag, Berlin, 2000, pp. 213–228.
31 C. Foti, C. Gianguzza, D. Piazzese and G. Trifiletti, *Chem. Speciation Bioavail.*, 2000, **12**, 41–52.
32 P. Cardiano, O. Giuffrè, L. Pellerito, A. Pettignano, S. Sammartano and M. Scopelliti, *Appl. Organomet. Chem.*, 2006, **20**, 425–435.
33 A. De Robertis, A. Gianguzza, O. Giuffrè, A. Pettignano and S. Sammartano, *Appl. Organomet. Chem.*, 2006, **20**, 89–98.
34 C. De Stefano, A. Gianguzza, O. Giuffrè, A. Pettignano and S. Sammartano, *Appl. Organomet. Chem.*, 2008, **22**, 30–38.
35 P. Cardiano, C. De Stefano, O. Giuffrè and S. Sammartano, *Biophys. Chem.*, 2008, **133**, 19–27.
36 R. Jirásko, M. Holcapek, L. Kolarova and T. S. Basu Baul, *J. Mass Spectrom.*, 2007, **42**, 918–928.
37 P. Surdy, P. Rubini, N. Buzás, B. Henry, L. Pellerito and T. Gajda, *Inorg. Chem.*, 1999, **38**, 346–352.
38 T. P. Lockhart and W. F. Manders, *Inorg. Chem.*, 1986, **25**, 892–895.
39 C. De Stefano, S. Sammartano, P. Mineo and C. Rigano, Computer tools for the speciation of natural fluids, in *Marine Chemistry—An Environmental Analytical Chemistry Approach*, ed. A. Gianguzza, E. Pelizzetti and S. Sammartano, Kluwer Academic Publishers, Amsterdam, 1997, pp. 71–83.
40 C. Bretti, C. De Stefano, C. Foti and S. Sammartano, *J. Solution Chem.*, 2006, **35**, 1227–1244.
41 H.-P. Abicht, K. Jurkschat, A. Tzschach, K. Peters, E.-M. Peters and H. G. von Schnering, *J. Organomet. Chem.*, 1987, **326**, 357–368.
42 G. Van Koten, J. T. B. H. Jastrzebski, J. G. Noltes, A. L. Spek and J. C. Schoone, *J. Organomet. Chem.*, 1978, **148**, 233–245.
43 M. Mehring, C. Löw, M. Schürmann and K. Jurkschat, *Eur. J. Inorg. Chem.*, 1999, 887–898.
44 P. G. Harrison, K. Lambert and T. J. King, *J. Chem. Soc., Dalton Trans.*, 1983, 363–369.